JCB Article

Mammalian GGAs act together to sort mannose 6-phosphate receptors

Pradipta Ghosh,[1] Janice Griffith,[2] Hans J. Geuze,[2] and Stuart Kornfeld[1]

[1]Department of Internal Medicine, Washington University School of Medicine, St. Louis, MO 63110
[2]Department of Cell Biology, University Medical Center and Institute of Biomembranes, Utrecht University, 3584 CX Utrecht, Netherlands

The GGAs (Golgi-localized, γ ear–containing, ADP ribosylation factor–binding proteins) are multidomain proteins implicated in protein trafficking between the Golgi and endosomes. We examined whether the three mammalian GGAs act independently or together to mediate their functions. Using cryo-immunogold electron microscopy, the three GGAs were shown to colocalize within coated buds and vesicles at the trans-Golgi network (TGN) of HeLa cells. In vitro binding experiments revealed multidomain interactions between the GGAs, and chemical cross-linking experiments demonstrated that GGAs 1 and 2 form a complex on Golgi membranes. RNA interference of each GGA resulted in decreased levels of the other GGAs and their redistribution from the TGN to cytosol. This was associated with impaired incorporation of the cation-independent mannose 6-phosphate receptor into clathrin-coated vesicles at the TGN, partial redistribution of the receptor to endosomes, and missorting of cathepsin D. The morphology of the TGN was also altered. These findings indicate that the three mammalian GGAs cooperate to sort cargo and are required for maintenance of TGN structure.

Introduction

The Golgi-localized, γ ear–containing, ADP ribosylation factor–binding protein (GGA) family of proteins includes three members in mammalian cells, numbered 1–3 (Boman et al., 2000; Dell'Angelica et al., 2000; Hirst et al., 2000; Poussu et al., 2000; Takatsu et al., 2000). These proteins have been implicated in mediating mannose 6-phosphate receptor (MPR) trafficking at the TGN. They share ∼35–45% sequence identity (Boman et al., 2000; Hirst et al., 2000) and have identical domain organizations with an NH_2-terminal Vps, Hrs, and STAM (VHS) domain, followed by a coiled-coil GGA and Tom (GAT) domain, a variable hinge region, and a COOH-terminal appendage that is homologous to the γ-appendage of adaptor protein 1 (AP-1). The three mammalian GGAs bind to an acidic cluster/dileucine-sorting motif on the cytoplasmic tails of the two MPRs via their VHS domains (Puertollano et al., 2001; Takatsu et al., 2001; Zhu et al., 2001). They also directly interact with the γ-appendage of AP-1 (Doray et al., 2002c) as well as clathrin (Puertollano et al., 2001; Zhu et al., 2001) via their hinge domains. Furthermore, GGAs 1 and 2 have been shown to colocalize with AP-1 within clathrin-coated vesicles (CCVs) and buds at the TGN (Doray et al., 2002c; Puertollano et al., 2003).

Despite these similarities, the three GGAs have several differences: (1) GGAs 1 and 3 are phosphorylated (Doray et al., 2002b), whereas GGA2 lacks this form of post-transcriptional modification; (2) GGAs 1 and 3 are regulated via an intramolecular autoinhibitory conformation (Doray et al., 2002b; Ghosh and Kornfeld, 2003), whereas GGA2 has not been shown to possess a similar regulatory mechanism; and (3) the crystal structures of the three VHS domains have revealed significant differences between the VHS domain of GGA2 and that of GGAs 1 and 3 in the loop between helices 6 and 7, which forms part of the ligand-binding pocket (Zhu et al., 2003).

Address correspondence to Stuart Kornfeld, Washington University School of Medicine, Dept. of Internal Medicine, 660 S. Euclid Ave., Box 8125, St. Louis, MO 63110. Tel.: (314) 362-8803. Fax: (314) 362-8826. email: skornfel@im.wustl.edu

P. Ghosh's present address is University of California, San Diego Medical Center, Department of Medicine, 200 West Arbor Drive, San Diego, CA 92103-8422.

Key words: trans-Golgi network; clathrin-coated vesicle; adaptor protein 1; siRNA; cryo-immunogold EM

Abbreviations used in this paper: AP-1, adaptor protein 1; ARF, ADP ribosylation factor; β-GalT, β-galactosyltransferase; CCV, clathrin-coated vesicle; CI-MPR, cation-independent MPR; DTSSP, 3,3′-dithiobis[sulfosuccinimidylpropionate]; EEA1, early endosomal antigen 1; GAT, GGA and Tom; GGA, Golgi-localized, γ ear–containing, ADP ribosylation factor–binding protein; MPR, mannose 6-phosphate receptor; RNAi, RNA interference; siRNA, small interfering RNA; VHS, Vps, Hrs, and STAM.

The structural similarities and functional redundancy between the GGAs raise the possibility that they work independently and that one member of the family might be able to compensate for the loss of the other(s) as in yeast (Black and Pelham, 2000). Alternatively, the three GGAs might act together in performing the sorting functions at the TGN. If the GGAs were to form a complex on the membrane, the resultant multivalency might enhance the recruitment of cargo molecules and accessory proteins involved in vesicle assembly. In this case, depletion of any one GGA molecule might cause maximal functional impairment.

In this work, we have used a variety of techniques to distinguish between the two possibilities. Our findings indicate that the three GGAs bind to each other to form a complex on the Golgi membranes and that each GGA is required for proper sorting of the MPRs. Further, knockdown experiments using RNA interference (RNAi) have revealed that the GGAs are required for maintenance of the TGN architecture.

Results

GGAs 1, 2, and 3 colocalize at the TGN

In our initial experiments, the three GGAs were localized with respect to each other using confocal microscopy. Fig. 1 illustrates the findings with HeLa cells cotransfected with plasmid DNA encoding myc-GGA1 and GGA2-HA (Fig. 1 A) or myc-GGA1 alone (Fig. 1 B). Intricate TGN patterns stained for both GGAs were imaged and examined for colocalization. The colocalization coefficient between red and green pixels representing myc-GGA1 and GGA2-HA, respectively, was 92% in Fig. 1 A, and that for myc-GGA1 and endogenous GGA2 in Fig. 1 B was 90%. Similar findings were observed with GGA2 and GGA3 (unpublished data). These results confirm the previous reports on GGA localization (Boman et al., 2000; Dell'Angelica et al., 2000; Hirst et al., 2000). As noted earlier (Boman et al., 2000), peripheral punctate structures labeled for either GGA showed poor overlap.

To determine whether the three GGA molecules function within separate clathrin-coated buds at the TGN or if they are within the same buds, we examined the distribution of endogenous GGAs 1, 2, and 3 in HeLa cells by means of cryoimmunogold EM. As shown in Fig. 2 D, GGA1 and GGA2 were found to colocalize within the same coated buds at the TGN. Fig. 2 E shows similar colocalization between GGAs 2 and 3. Stably transfected HeLa cells expressing myc-GGA1 were used to demonstrate colocalization between myc-GGA1 and endogenous GGA3 (Fig. 2 A). Triple-labeling experiments with gold particles of three different sizes showed that all three GGAs colocalize within the same coated buds and vesicles at the TGN (Fig. 2, B and C). A quantitative evaluation of the GGA-labeled clathrin-coated vesicles and buds in the triple labeled cryosections revealed that 38.5% of these structures contained two GGAs, and 13% contained all three GGAs, giving a total of 51.5% with two or three GGAs. Because of efficiency limitations of the immunogold labeling procedure, these values probably represent significant underestimates of the actual degree of colocalization.

These observations are consistent with the model where the three GGAs work within the same bud to concentrate cargo in a cooperative fashion. However, because only a single type of GGA was detected in some of the buds, we can't rule out the possibility that the individual members of the family might also nucleate their own buds.

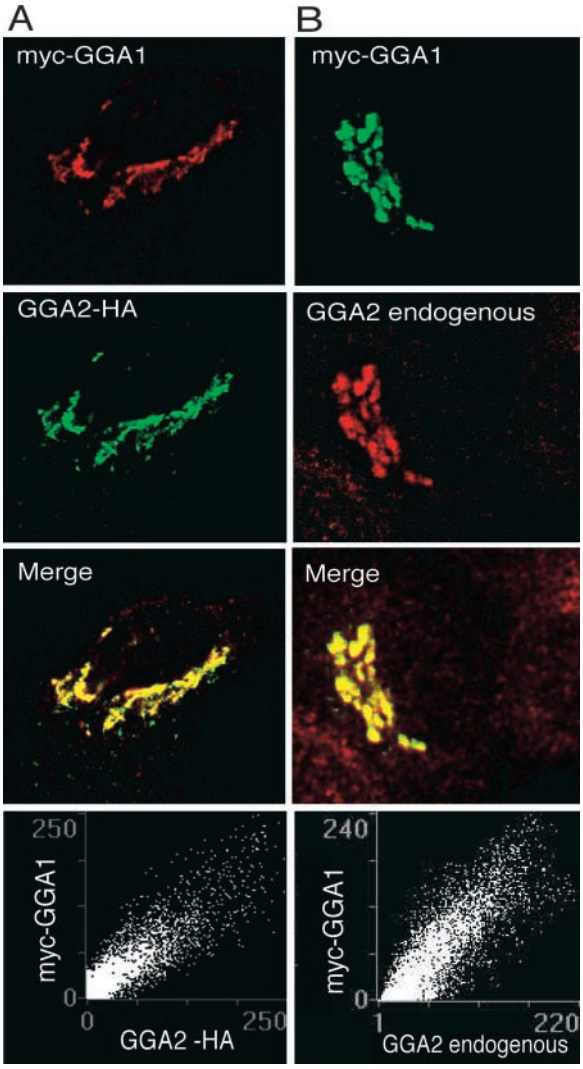

Figure 1. **GGAs 1 and 2 colocalize on the TGN.** (A) HeLa cells cotransfected with plasmid DNA encoding myc-GGA1 and GGA2-HA were fixed 48 h after transfection, and double-labeled confocal immunofluorescence was performed using anti-c-myc to detect myc-GGA1 (red) and anti-HA to detect GGA2-HA (green). Confocal images were analyzed and merged using software programs as described in Materials and methods. Scattergram of red and green pixels were plotted on a graph to obtain the colocalization coefficient between myc-GGA1 and GGA2-HA. (B) HeLa cells transfected with plasmid DNA encoding myc-GGA1 were fixed 48 h after transfection and processed for confocal immunofluorescence using anti-c-myc to detect myc-GGA1 (green) and rabbit polyclonal anti-GGA2 antibody to detect endogenous GGA2 (red). A scattergram was plotted as in A to look for colocalization of the red and green pixels.

Direct and multidomain interaction between the GGAs

The GGAs were initially characterized as monomeric cytosolic proteins based on their behavior on gel filtration chromatography and sucrose gradients (Dell'Angelica et al., 2000; Hirst et al., 2000). However, their colocalization on coated buds and vesicles of the TGN indicated that they might form a complex on the membrane, in which case they should be ca-

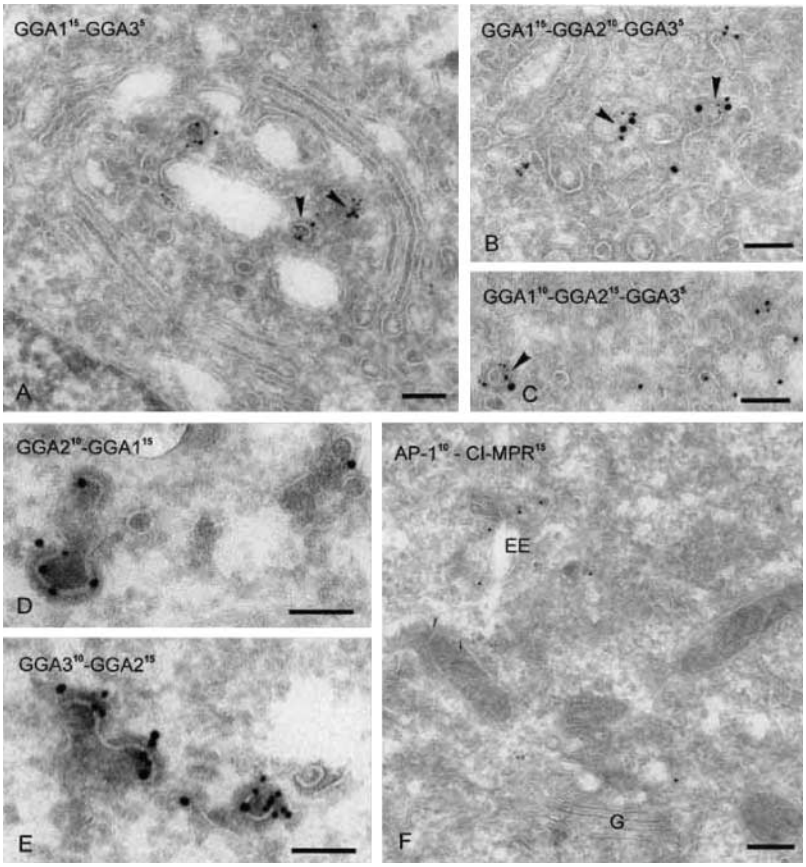

Figure 2. **GGAs 1, 2 and 3 colocalize within the same coated buds at the TGN.** Electron micrographs of immunogold-labeled cryosections showing the colocalization of GGAs (A–E) and the distribution of CI-MPR and AP-1 in the trans-Golgi area of a GGA1 siRNA cell (F). (A–C) HeLa cells expressing myc-tagged GGA1. Using antibodies against myc, GGA2, and GGA3, double- and triple-labeling experiments with 5-, 10-, and 15-nm gold show that all three GGAs colocalize to coated pits and vesicles at the TGN (arrowheads). D and E show the colocalization of endogenous GGA1, 2, and 3 at coated buds on the TGN in HeLa cells. (F) AP-1 and CI-MPR double immunolabeling in a GGA1-depleted HeLa cell. G, Golgi stack; EE, early endosome. Bars: (A–E) 100 nm, (F) 250 nm.

pable of binding to each other. First, we tested the various GGAs for interactions among themselves using in vitro binding assays. GST-fused GGA proteins expressed and purified from bacteria were immobilized on glutathione-Sepharose beads and tested for binding to GGAs immunopurified from a baculovirus expression system. Each GGA molecule interacted with the two other family members, but not with GST (Fig. 3 A). In the case of GGA1, this interaction appeared not to be influenced by the phosphorylation status of the serine residue at position 355 because myc-GGA1wt behaved similarly to myc-GGA1 D358A (Fig. 3 A, middle). This mutation impairs casein kinase 2–mediated phosphorylation at serine 355 (Doray et al., 2002b; Ghosh and Kornfeld, 2003). GGA2 and GGA3 also bound to themselves. In some experiments, GGA1 did not bind to itself, but in other experiments such binding was detected (unpublished data). This suggests that GGA1 interacts better with the other GGAs than it does with itself. Because immunopurified proteins were used in all the experiments, we conclude that these were direct interactions.

Next, we sought to determine the domain(s) responsible for mediating the GGA2–GGA3 interaction. Immunopurified myc-GGA3 was pulled down by intact GGA2 as well as constructs consisting of the VHS domain, the VHS–GAT domains, and the ear domain (Fig. 3 B). This indicates that the interaction is mediated via multiple domains. Because the GST-GGA2 fl (full-length), GST-GGA2 fl Δear (deleted ear domain), and GST-GGA2 VHS-GAT proteins (Fig. 3 B, lanes 3, 4, and 6) purified from bacterial lysates contained multiple breakdown products, it was not possible to compare the binding ability of these constructs in a quantitative manner.

GGAs 1 and 2 form a complex upon recruitment onto Golgi-enriched membranes

Next, we tested whether the GGAs form a complex after recruitment onto Golgi membranes via ADP ribosylation factor GTP (ARF–GTP; Puertollano et al., 2001). As shown in Fig. 4 A, we first confirmed GTPγS-mediated recruitment of GGA1 and GGA2 from bovine adrenal cytosol onto rat liver Golgi-enriched membranes. In Fig. 4 B, the chemical cross-linking reagent 3,3′-dithiobis[sulfosuccinimidylpropionate] (DTSSP) was used to cross-link the proteins recruited onto the membrane (as described in Materials and methods). The control and cross-linked membranes were solubilized in the presence of detergent, and GGAs 1 and 2 were immunoprecipitated from different aliquots. Immunoprecipitation of GGA2 from the cross-linked membranes resulted in recovery of GGA1 as well (Fig. 4 B, lane 9, top) and vice versa (Fig. 4 B, lane 8, bottom). Coimmunoprecipitation did not occur in the absence of chemical cross-linking (Fig. 4 B, compare lanes 8 and 9 with lanes 2 and 3). Cytosolic GGAs failed to coimmunoprecipitate (Fig. 4 B, lanes 4–6 and lanes 10–12) with or without cross-linking, demonstrating that the GGA1–GGA2 complex is generated only on membranes. It is unlikely that this result is an artifact of nonspecific cross-linking because an abundant and unrelated Golgi-resident protein, mannosidase II, was not detected in the immunoprecipitates after DTSSP treatment (unpublished data). It was not possible to analyze the immunoprecipitates for the presence of GGA3 because the monoclonal anti-GGA3 antibody used in our experiments does not react with the bovine form of this GGA.

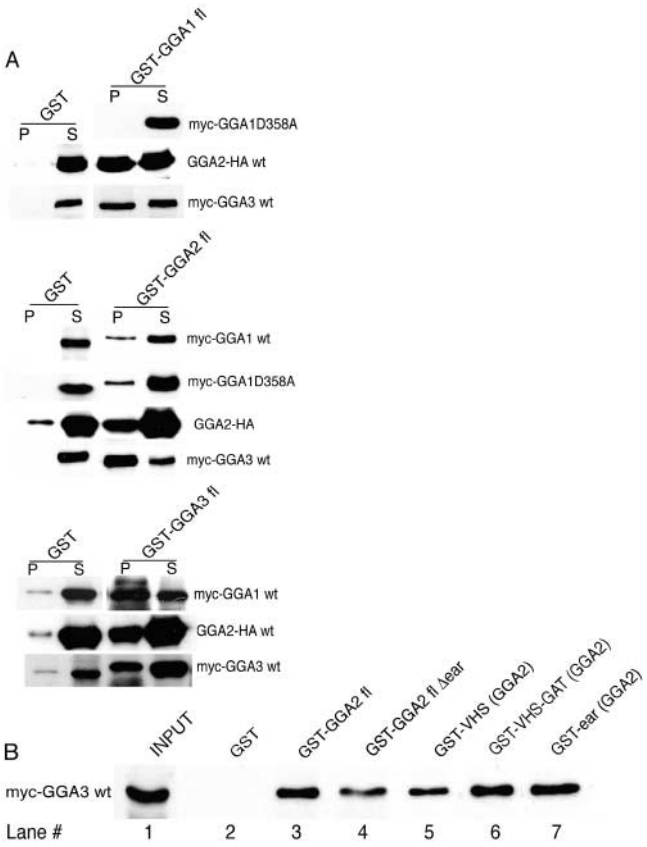

Figure 3. **Direct interaction of GGAs with each other in in vitro assays.** (A) GST-fused full-length GGA1, GGA2, and GGA3 proteins prebound to glutathione-Sepharose beads were used in binding assays with affinity-purified myc-GGA1wt, myc-GGA1 D358A, myc-GGA3, and GGA2-HA as described in Materials and methods. GST alone was used as a negative control. The bound proteins were eluted by boiling in SDS sample buffer and were subjected to SDS-PAGE and Western blotting using anti-c-myc or anti-HA mAbs to detect GGAs1/3 and GGA2, respectively. P, pellet; S, supernatant. (B) GST-fused GGA2 proteins (full-length, GST-GGA2flΔear, GST-VHS, GST-VHS+GAT, and GST-ear; see Materials and methods for aa sequences) prebound to glutathione-Sepharose beads were used in binding assays with affinity-purified myc-GGA3 wild type. The bound GGA3 was eluted in SDS sample buffer, and an aliquot (20%) of the same was subjected to SDS-PAGE and Western blotting with anti-c-myc mouse mAb. The above result is one of two independent experiments.

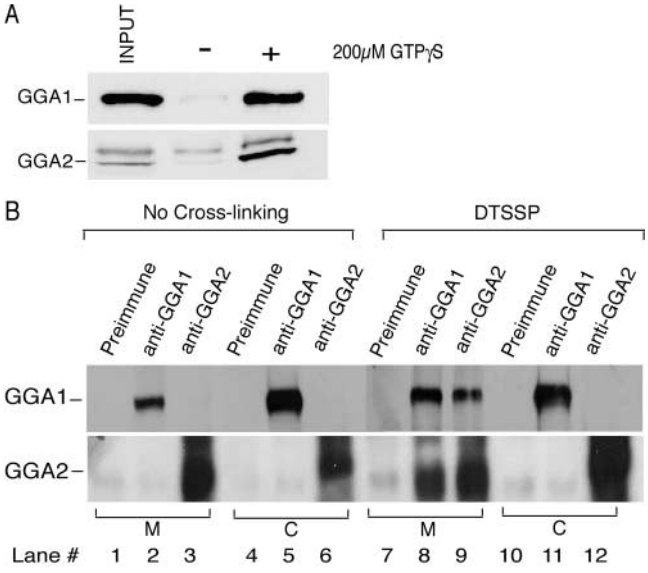

Figure 4. **GGAs form a complex upon recruitment onto Golgi-enriched membranes.** (A) Bovine adrenal cytosolic GGAs were recruited onto rat Golgi-enriched membranes in the presence or absence of GTPγS as described in Materials and methods. The membrane-associated proteins were boiled in SDS sample buffer and subjected to SDS-PAGE and Western blotting with either anti-GGA1 or anti-GGA2 pAbs. (B) Recruitment reactions were scaled up and performed as above, followed by chemical cross-linking of membrane-associated proteins with DTSSP as described in Materials and methods. The cross-linked proteins were then isolated by solubilizing the membranes with detergent and were coimmunoprecipitated using either rabbit preimmune sera (negative control) or anti-GGA1 or GGA2 affinity-purified antibodies. Immunoprecipitated proteins were subjected to SDS-PAGE and Western blotting to detect GGA1 and GGA2. A 2-mg aliquot of cytosol (supernatants from the recruitment reactions) was also subjected to cross-linking and coimmunoprecipitation as described in the case of membranes. M, membrane; C, cytosol. Of note, GGA1 migrated slower than expected for its calculated molecular weight.

Depletion of any one GGA results in a partial decrease in the levels of the others

If the GGAs function at the TGN as a complex, knocking down any one of the family members might destabilize the complex and result in maximal functional impairment. On the other hand, if they work independently, knocking down any one of them should only result in partial impairment or no impairment at all if the other members can compensate for the missing GGA molecule, as reported for yeast GGAs (Dell'Angelica et al., 2000; Hirst et al., 2000). To address this issue, the individual GGA genes in HeLa cells were post-transcriptionally silenced using a plasmid-based RNAi technique (Brummelkamp et al., 2002). As controls, we used RNAi targeting of the γ-subunit of AP-1 or cells transfected with p-Super vector alone. Fig. 5 A demonstrates that all four proteins targeted by the specific small interfering RNA (siRNA) were significantly depleted 52 h after transfection, as determined by quantitative Western blotting. A surprising finding was that knocking down any one GGA caused a significant partial decrease in the levels of the other two (Fig. 5, B–D). In the setting of transfection efficiencies ranging from 85–95%, the level of GGA1 was significantly decreased in GGA2 siRNA and GGA3 siRNA cells (50 and 47%, respectively) in addition to the expected depletion in GGA1 siRNA cells (Fig. 5 C). Cotransfection of a RNAi-resistant form of wild-type GGA1 into the GGA1 siRNA cells restored the level of GGAs 2 and 3 back to normal (Fig. 5 B, compare lane 6 with lane 3). The partial decrease in the other GGAs when any one of them was knocked down was a selective process, as this was not associated with a change in the level of AP-1, the cation-independent MPR (CI-MPR), β-galactosyltransferase (β-GalT), p63, an ER marker, or actin (Fig. 5 B).

To evaluate the possibility of proteasome-mediated degradation, the siRNA cells were incubated in the presence or absence of 25 μM carbobenzoxy-L-leucyl-L-leucyl-L-leucinal (MG-132), a cell-permeable proteasome inhibitor, for 10 h at 37°C, and the cell lysates were subjected to Western blotting to detect the levels of the various GGAs. As shown in the top of Fig. 5 D, expression levels of GGA1 were normal-

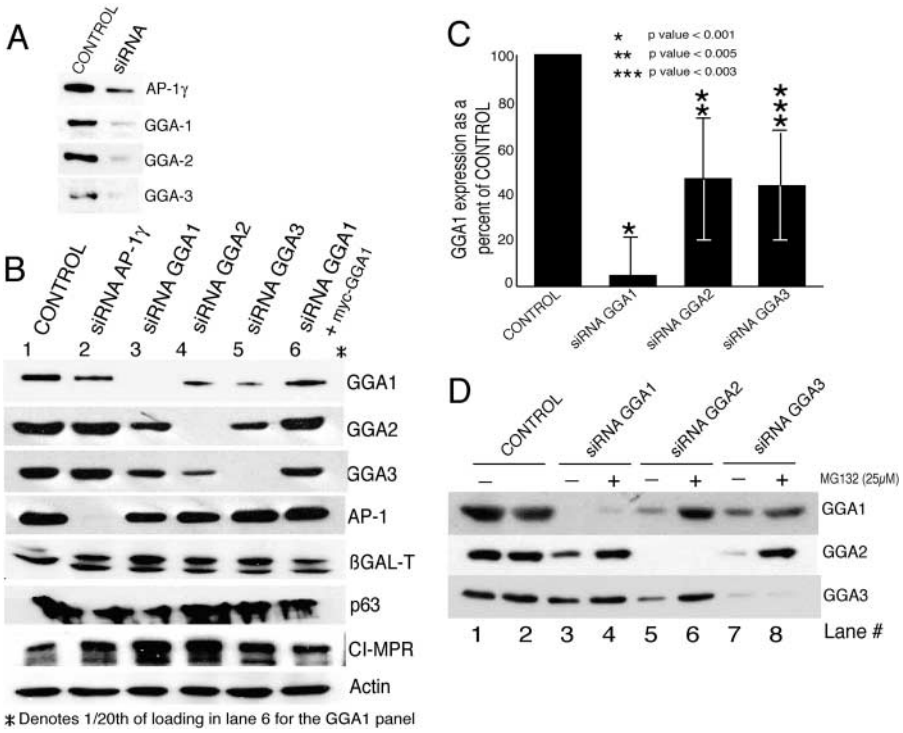

Figure 5. **Post-transcriptional silencing of GGAs 1, 2, and 3.** (A) HeLa cells transfected with either empty vector (control) or plasmid DNA encoding antisense siRNAs targeting the three GGAs or AP-1γ were harvested 56 h after transfection, and equal aliquots (25 μg) of the cell extracts were subjected to SDS-PAGE and Western blotting with appropriate antibodies to evaluate the efficiency of knockdown achieved. (B) 25-μg Aliquots of cell extracts prepared as in the above experiment were subjected to SDS-PAGE and Western blotting to detect the three GGAs, AP-1, and various marker proteins as indicated in the figure. For lane 6, HeLa cells were cotransfected with GGA1 siRNA plasmid and RNAi-resistant myc-GGA1 as described in Materials and methods. Loading in the first panel of lane 6 was 1/20th of the other lanes because the myc-GGA1 was greatly overexpressed. (C) Level of expression of GGA1 in control cells (plasmid only), GGA1 siRNA, GGA2 siRNA, and GGA3 siRNA cells was detected by Western blotting of cell extracts and was quantitated using a Kodak band densitometer. The amount of GGA1 in each of the cell lines was expressed as a percentage of the control. Error bars represent the values obtained from six independent sets of experiments. P-values were calculated using Sigma Plot. (D) HeLa cells transfected with either vector alone (control) or various siRNA GGA plasmids were subjected to treatment with 25 μM MG132 in DMSO (+) or with DMSO alone (−) for 10 h before harvest. Equal aliquots (33 μg) of cell extracts were subjected to SDS-PAGE and Western blotting to detect the levels of expression of the three GGA proteins.

ized in GGA2 siRNA and GGA3 siRNA cells treated with MG-132. Similarly, the levels of GGA2 were rescued in GGA1 siRNA and GGA3 siRNA cells incubated with the proteasome inhibitor (middle), and the levels of GGA3 returned to normal in GGA1 siRNA and GGA2 siRNA cells when treated with MG-132 (bottom). As expected, the MG-132 treatment had essentially no effect on the particular GGA that was targeted by the siRNA.

Morphology of the GGA-depleted cells

Overexpression of the various GGAs is known to cause structural changes in the Golgi. At moderate levels, it causes compaction of the TGN (Poussu et al., 2000), whereas at higher levels it causes fragmentation and/or vacuolation of the Golgi (Takatsu et al., 2000) and redistribution of various TGN markers (Boman et al., 2000). Therefore, it was proposed that GGAs may be responsible for maintenance of Golgi architecture, possibly by preserving the integrity of the Golgi stacks (Takatsu et al., 2000; Poussu et al., 2001) and/or regulating Golgi vesiculation during trafficking (Boman et al., 2000). The siRNA-treated cells allowed us to address these issues in a system that avoids the problems encountered when proteins are overexpressed. Using immunofluorescence of a variety of subcellular markers, we found striking alterations in the morphology of the GGA-depleted cells. As shown in Fig. 6 (E, G, and I), GGA depletion resulted in β-GalT, a trans-Golgi marker in HeLa cells (Strous et al., 1983; Nilsson et al., 1993), being present on extensive ribbonlike tubulations extending throughout the cell rather than in its usual compact perinuclear polarized location (Fig. 6 A). In contrast, AP-1 knockdown did not alter the trans-Golgi architecture as marked by the unaltered β-GalT staining (Fig. 6 C), consistent with an earlier report (Meyer et al., 2000). Giantin, which is present in all the Golgi cisternae but concentrated in the middle cisternae (Martinez-Menarguez et al., 2001), was unperturbed in these cells (Fig. 7, D–I). However, prolonged culture of GGA-silenced cells resulted in disruption of the entire Golgi and cell death (Fig. 7, J–O). β-GalT became undetectable after 90 h by immunofluorescence (Fig. 7 M) as well as by Western blotting (unpublished data).

The CI-MPR in the GGA knockdown cells was mostly detected in peripheral punctate structures that failed to colocalize with the β-GalT–stained tubules (Fig. 6, F, H, and J). The CI-MPR staining in AP-1–silenced cells also showed an increase in peripheral punctate distribution as reported earlier (Meyer et al., 2000; Fig. 6 D and Fig. 9 D). To better define the subcellular localization of CI-MPR in the knockdown cells, the cells were double labeled with early endosomal antigen 1 (EEA1), a marker for early endosomes, and CI-MPR. Fig. 8 (G–I) shows that the CI-MPR–labeled structures, sometimes tubular in appearance, colocalized with EEA1 in the GGA1 knockdown cells. A similar colocalization was seen in AP-1 knockdown cells (Fig. 8, D–F), and is in agreement with findings in fibroblasts derived from AP-1 μ1 knockout mice (Meyer et al., 2000). EEA1 and the CI-MPR were not colocalized in the control cells (Fig. 8, A–C). In the GGA1 siRNA cells, AP-1 was depleted from the Golgi and detected on the CI-MPR–containing tubular processes that appear to extend from the early endosomal compartments (Fig. 9, E and F).

When the GGA1 knockdown cells were viewed at a higher resolution using EM, most of the trans-Golgi was found displaced from its usual position close to the stacks, and fewer

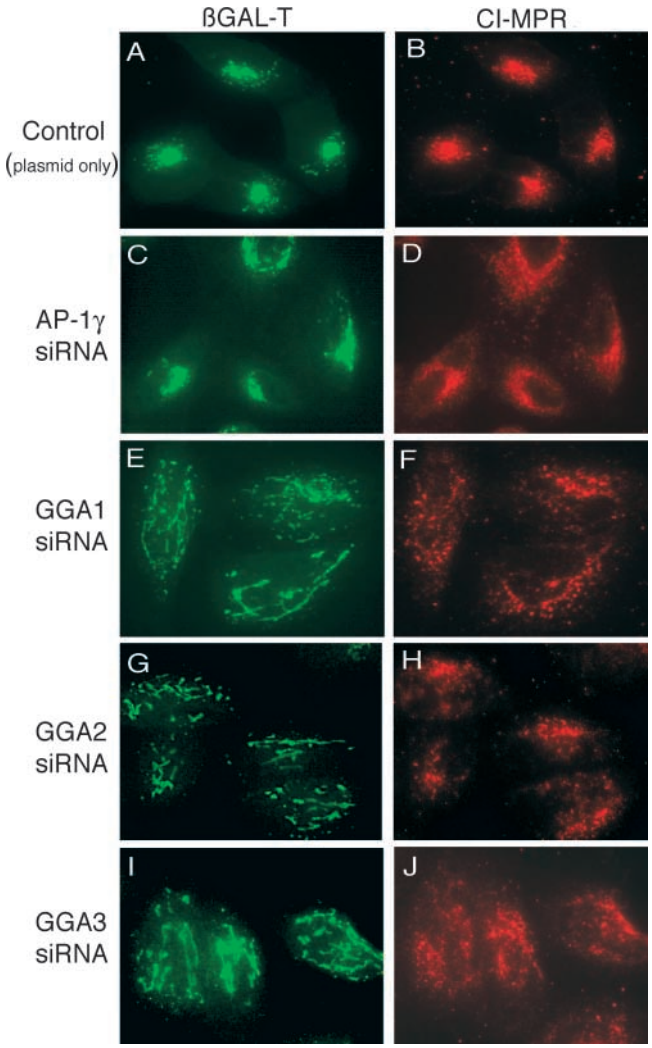

Figure 6. **Morphology of GGA1 knockdown cells.** HeLa cells were transfected with plasmid DNA encoding either vector only (A and B; control) or siRNAs directed against AP-1γ (C and D), GGA1 (E and F), GGA2 (G and H), and GGA3 (I and J) as described in Materials and methods. Cells were harvested 56 h after transfection and processed for double-labeled immunofluorescence with anti-β-GalT (green) and anti-CI-MPR (red).

CCVs were seen in the Golgi area (Fig. 2 F). The Golgi stacks were intact. Quantitation of these immunogold experiments showed that the content of CI-MPR in the TGN was significantly reduced (Table I). This was most striking in the TGN-associated CCVs, where the level of CI-MPR was decreased by 75%. The number of AP-1–positive, TGN-associated CCVs in the GGA1 knockdown cells was decreased by almost 50%. Although the total content of CI-MPR in identifiable endosomes was similar to that observed in control cells, the receptor was less abundant in the tubules/vesicles and more concentrated in the internal membranes. The significance of this shift is not clear at this point. In addition, there was a significant increase in the amount of CI-MPR in scattered tubules/vesicles located >500 nm from the endosomal central vacuoles. These data are consistent with the immunofluorescence experiments showing a shift of the CI-MPR from the TGN to peripheral punctate structures.

Golgi functions in the absence of GGAs

Cathepsin D sorting in GGA knockdown cells. Because GGAs are believed to have a role in sorting of MPRs at the TGN (Puertollano et al., 2001; Zhu et al., 2001; Doray et al., 2002a), we tested the ability of the siRNA-treated HeLa cells to target newly synthesized cathepsin D to lysosomes. This targeting is an MPR-dependent process. The cells were labeled with [^{35}S]Met/Cys for 1 h, and then were chased for 4 h in the presence of 5 mM mannose 6-phosphate to prevent reuptake of secreted enzyme. Intracellular and secreted cathepsin D were immunoprecipitated and quantitated as a percentage of the total cathepsin D (Table II). In transiently transfected siRNA cells, knocking down any one of the GGAs caused striking missorting of cathepsin D in the presence of 5 mM mannose 6-phosphate (81% secretion vs. 48% by control cells). As demonstrated before, AP-1 knockdown cells also failed to sort the newly synthesized lysosomal hydrolase (Meyer et al., 2001; Hirst et al., 2003). This is in contrast to the findings in yeast, where the two GGAs (1 and 2) are redundant in their ability to sort carboxypeptidase Y to the vacuole (Dell'Angelica et al., 2000; Hirst et al., 2000).

We also generated stable GGA1 siRNA and GGA2 HeLa cell lines that express ~30% of the control levels of the targeted proteins as determined by Western blotting (unpublished data). These cells demonstrated partial missorting of cathepsin D in the presence of 5 mM mannose 6-phosphate (67 and 68% secretion vs. 53% by control cells). The effect was modest, presumably due to the failure of complete knockdown. These stable cell lines had normal β-GalT and giantin staining of their Golgi as assessed by immunofluorescence. Therefore, at 30% of control levels of expression, the residual GGAs appear to be sufficient for maintenance of Golgi structure, whereas MPR-mediated sorting is partially impaired.

N-linked oligosaccharide processing in GGA knockdown cells. Because several of the enzymes necessary for proper processing of Asn-linked oligosaccharides are localized within the trans-Golgi, we assessed Asn-linked glycan processing in transient and stably transfected GGA1 knockdown cells. Using sequential lectin column chromatography of 2-(^{3}H)mannose-labeled cellular glycopeptides, first on Con A–Sepharose to separate complex from high mannose oligosaccharide glycopeptides, followed by fractionation of the complex species on RCA-Sepharose to separate the sialylated from nonsialylated species, we found no differences between the control and GGA1 knockdown cells (unpublished data). These results agree with those reported earlier (Stults et al., 1989), where a disrupted trans-Golgi was completely functional with respect to the fidelity of Asn-linked glycosylation. Similar results were obtained with GGA2 siRNA cells (unpublished data).

Correction of knockdown morphology. If the altered morphology of the cells is entirely due to depletion of endogenous GGAs, the phenotype should be reversed when the depleted GGA is restored by transfection of the missing GGA gene. To express myc-GGA1 in the GGA1 siRNA cells, we mutated a single nucleotide within the 21-bp target sequence to confer RNAi resistance while maintaining the wild-type amino acid sequence. HeLa cells were then cotransfected with GGA1 siRNA plasmid DNA and the RNAi-resistant myc-GGA1 pcDNA 3.1 (as described in Materials and methods). In every cell expressing the RNAi-resistant wild-type

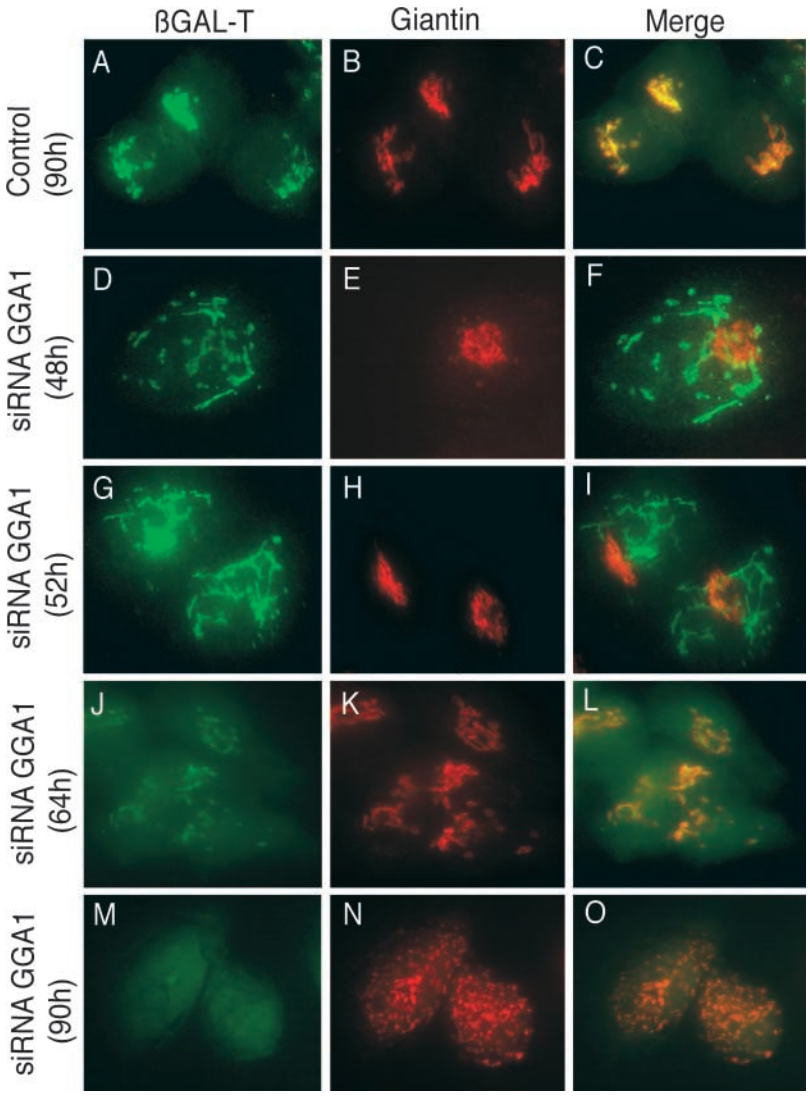

Figure 7. **Disruption of Golgi architecture in GGA knockdown cells.** HeLa cells transfected with plasmid DNA expressing GGA1 siRNA were harvested at the indicated times after transfection and processed for double-labeled immunofluorescence with antibodies against β-GalT (green) and giantin (red).

myc-GGA1, β-GalT and CI-MPR exhibited perinuclear Golgi staining (Fig. 10, C and D, and A and B, respectively). The endogenous levels of GGAs 2 and 3 were normalized (Fig. 5 B, lane 6), and their localization, which had been displaced from the Golgi to the cytosol, was restored (Fig. 10, E–H). No correction of the morphology was observed when RNAi-resistant GGA2-HA was transfected into GGA1 siRNA cells (unpublished data). Incubation of the GGA1 knockdown cells with the proteasome inhibitor MG132, which prevents the degradation of the other GGAs (Fig. 5 D), increased the cytosolic staining of GGA2 and GGA3, but failed to restore their Golgi localization (unpublished data).

Discussion

The findings presented in this paper provide evidence that the three members of the mammalian GGA family act together to mediate the sorting of MPRs into transport vesicles at the TGN. The experiments also reveal a role for the GGAs in maintaining the architecture of the trans-Golgi and TGN. Using confocal microscopy, the three GGAs were found to colocalize in the TGN, and cryo-immunogold EM showed that all three GGAs were present in the same clathrin-coated buds and vesicles. These results are in agreement with prior reports on the colocalization of the GGAs at the TGN (Boman et al., 2000; Dell'Angelica et al., 2000; Hirst et al., 2000).

Although these morphologic findings are consistent with the three GGAs acting together to package cargo into transport vesicles, they do not exclude the possibility that the various GGAs function independently. To address this issue, we performed binding experiments demonstrating that the various GGAs bind to each other, consistent with the GGAs forming a complex on the membrane. Further evidence for complex formation was obtained by cross-linking experiments after recruitment of the GGAs onto Golgi-enriched membranes.

These experiments showed that GGA1 and GGA2 could be cross-linked on the membrane, but not in the cytosol. Due to the inability to detect GGA3 in bovine adrenal cytosol, we were unable to determine whether GGA3 was also present in the Golgi-associated complex. However, this is likely in view of the direct interaction of GGA3 with the other GGAs in the pull-down assays.

Together, these findings indicate that the individual GGAs are recruited as monomers from the cytosol onto the Golgi in an ARF–GTP-dependent manner, and then form a complex that subsequently interacts with AP-1 at regions of

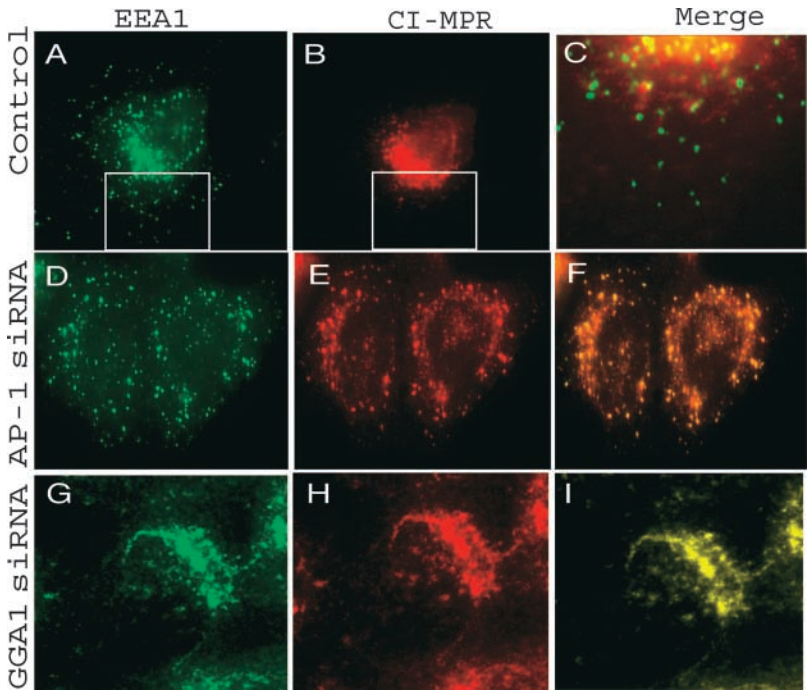

Figure 8. **Redistribution of CI-MPR to peripheral EEA1-positive compartments.** HeLa cells transfected with AP-1 siRNA or GGA1 siRNA were double labeled with anti-CI-MPR (red) and anti-EEA1 (green). C is a blow-up of the boxed areas in A and B.

clathrin-coated bud formation (Doray et al., 2002c). The multivalency of the assembled complex could serve to enhance the recruitment of cargo molecules and accessory proteins involved in vesicle formation.

The precise nature of the interactions of the GGAs with each other remains to be explored. Our preliminary findings indicate that multiple domains are involved, as both the VHS and the ear domains of GGA2 bind GGA3. Potentially, the VHS domain of GGA2 could bind to the internal acidic cluster/dileucine motif within the hinge segment of GGA3 (Doray et al., 2002b). Likewise, the ear domain of GGA2, which is homologous to the γ-appendage of AP-1, could bind to the hinge domain of GGA3 (Doray et al., 2002c). Furthermore, crystal structures of the GAT domains of the GGAs have revealed a conserved binding site that is predicted to interact with coiled-coil domain-containing proteins (Suer et al., 2003). Thus, the GAT domains that have a predominantly coiled-coil structure might contribute to inter-GGA binding by interacting with each other. Because the various domains of the GGAs can be separately expressed, it should be possible to analyze the nature of these interactions in vitro. While this manuscript was in preparation, Wakasugi et al. (2003) re-

Table I. **Quantitative distribution of CI-MPR in HeLa cells**

	Control plasmid treated cells	GGA1 siRNA treated cells	*t* test
	%	%	
TGN (total)	24.4	11.6	P = 0.004
Tubules/vesicles	17.6	10.0	P = 0.03
CCVs	6.8	1.6	P = 3.8 × E − 5
Endosomes (total)	46.0	46.2	
Tubules/vesicles	27.1	14.4	P = 0.002
Vacuoles	16.1	31.0	P = 4.6 × E − 6
Limiting	12.9	15.0	
Internal	3.2	16.0	
CCVs	2.8	0.8	
Scattered (total)	13.0	27.7	P = 6.2 × E − 8
Tubules/vesicles	9.3	25.1	
CCVs	3.7	2.6	
Plasma membrane	9.1	5.4	P = 0.04
Others	7.5	9.6	

Percentages of CI-MPR immunogold particles on the compartments listed. For each condition, 1,000 gold particles were randomly counted in the electron microscope at 12 K. The TGN consisted of noncoated tubules and vesicles and of clathrin-coated vesicles/buds (CCVs) within a distance of 55 nm from the trans-most Golgi cisternae. Endosomes were vacuoles containing internal and limiting membranes, and were surrounded by noncoated tubules and vesicles and by CCVs within 500 nm from the central vacuoles. The other tubules, vesicles, and CCVs outside these distances comprise the group "scattered." "Other" is ER, Golgi stacks, vesicles at the Golgi cis- and lateral faces, and cytosol.

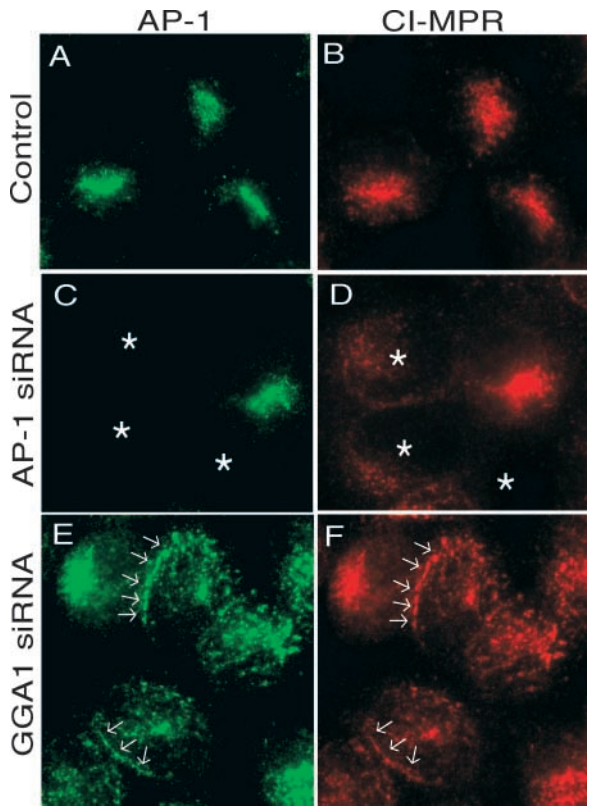

Figure 9. **AP-1 and CI-MPR colocalize within peripheral structures.** HeLa cells transfected with vector alone (A and B; control), AP-1 siRNA (C and D) and GGA1 siRNA (E and F) were harvested 56 h after transfection and immunostained for AP-1 (green) and CI-MPR (red). Asterisks designate cells with AP-1 knockdown. Arrows highlight areas where AP-1 and the CI-MPR colocalize on tubular processes.

ported that the GGA3 short form is the predominant form of GGA3 expressed in cell lines and all tissues except brain. This form has a unique VHS domain that lacks a region around helix 6 implicated in binding acidic cluster/dileucine motifs (Misra et al., 2002; Shiba et al., 2002). Even though this form of GGA3 is unlikely to be directly involved in the cargo protein recognition, it was found on similar TGN membranes as GGA1 by immunofluorescence. Our analyses indicate that the

Table II. **Sorting of cathepsin D in transiently transfected siRNA cells in the presence of 5 mM mannose 6-phosphate**

Constructs		Percent sorted	Percent secreted
Control (plasmid only)	$n = 3$	52.5	47.5
AP-1γ siRNA	$n = 2$	21.5	78.5
GGA1 siRNA	$n = 2$	18.4	81.6
GGA2 siRNA	$n = 2$	19.5	80.5
GGA3 siRNA	$n = 2$	19.5	80.5

HeLa cells transfected with the various plasmids listed in the table above were labeled with [^{35}S]methionine to assess the cellular efficiency in sorting newly synthesized cathepsin D in the presence of 5 mM mannose 6-phosphate. Cathepsin D within the cells (sorted) and in the medium (secreted) was immunoprecipitated and subjected to nonreducing SDS-PAGE, followed by autoradiography and quantitation as described in Materials and methods. Both fractions were expressed as a percentage of the total cathepsin D labeled during the pulse phase. *n* denotes the number of independent experiments performed.

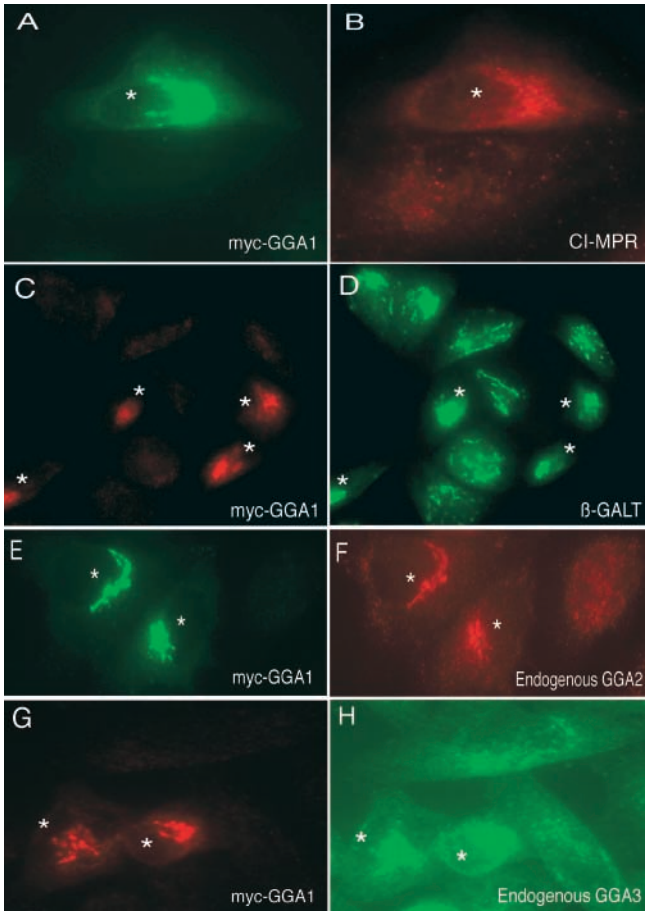

Figure 10. **Prevention of morphological changes in GGA1 knockdown cells by transfection of RNAi-resistant myc-GGA1.** HeLa cells were cotransfected with GGA1 siRNA and RNAi-resistant myc-GGA1 as described in Materials and methods. 56 h after transfection, the cells were harvested for double-labeled immunofluorescence to detect myc-GGA1 (green) and CI-MPR (red; A and B); myc-GGA1 (red) and β-GalT (green; C and D); myc-GGA1 (green) and endogenous GGA2 (red; E and F); and myc-GGA1 (red) and endogenous GGA3 (green; G and H). Asterisks indicate the cells expressing transfected myc-GGA1.

function of the GGA3 short form could be to stabilize the complex formed by the three GGAs on the TGN membranes.

Further evidence that the GGAs act together was obtained with the post-transcriptional gene silencing experiments using RNAi to knockdown the individual GGAs. At the morphological level, the loss of any one GGA resulted in the others being redistributed from the TGN to the cytosol (Fig. 10). This is consistent with the three GGAs needing to form a complex on the TGN membrane to maintain a stable association with this organelle. A key finding was that the knockdown of any one GGA was associated with maximal missorting of cathepsin D, a process that is dependent on the function of the MPRs. In contrast to yeast, where the two GGAs compensate for each other's absence (Dell'Angelica et al., 2000; Hirst et al., 2000), the requirement for all three GGAs to maintain the MPR sorting function supports the notion that the GGAs act together in mammalian cells. This is not the only difference between the yeast and mammalian GGA proteins. Although the mammalian GGAs co-

operate with AP-1 in TGN-to-endosome transport (Doray et al., 2002c), yeast GGAs and AP-1 appear to mediate independent trafficking pathways (Black and Pelham, 2000).

It is curious that the knockdown of any one GGA was associated with a partial decrease in the levels of the other GGAs. Levels of the nontargeted GGAs could be restored by transfection of the silenced GGA or by treatment of the cells with the proteasome inhibitor MG132. The mechanism whereby depletion of one GGA results in enhanced proteasomal degradation of the other GGAs is not clear at this point. Perhaps an increase in the cytosolic pool of GGAs in the absence of membrane complex formation triggers this degradative pathway.

As mentioned earlier in this section, the hypersecretion of cathepsin D by the GGA knockdown cells is most likely due to disordered MPR trafficking. In these cells, the CI-MPR was partially redistributed from the TGN to EEA1-positive early endosomal compartments, similar to what has been observed in AP-1 knockout cells (Meyer et al., 2000). Even more striking was the significant exclusion of the CI-MPR from the CCVs of the TGN. This alteration in the steady-state distribution of the CI-MPR could be accounted for by several mechanisms. We have proposed that GGAs may bind MPRs in the trans-Golgi and bring them to AP-1–containing clathrin-coated membranes at the TGN, where the MPRs are then transferred to AP-1 (Doray et al., 2002c; Ghosh and Kornfeld, 2003). This was based on the finding that mutant MPRs that are incapable of binding to GGAs, but not impaired in binding to AP-1, are poorly incorporated into AP-1-containing clathrin-coated buds and vesicles at the TGN. In the absence of binding to membrane-associated GGAs, the MPRs may exit the Golgi via secretory pathways to the cell surface where they would be rapidly internalized into early endosomes. Not only would this decrease the packaging of the MPRs into AP-1 vesicular carriers at the TGN, it might shift the steady-state distribution of the MPRs toward the early endosome compartment. This would occur if the GGAs normally retain the MPRs in the terminal Golgi compartments and prevent premature exit via the plasma membrane–targeting pathway. In addition, GGAs, like AP-1, might be involved in early endosome-to-TGN retrieval of the MPRs, as well as in anterograde transport from the TGN. GGAs have been localized to early endosome-like punctate peripheral structures (Boman et al., 2000; Dell'Angelica et al., 2000; Hirst et al., 2000), although in our immuno-EM analyses, GGAs have only occasionally been found on endosomes. It has also been reported that the COOH-terminal dileucine motif of the cation-dependent MPR is essential for retrograde trafficking (Tikkanen et al., 2000) and the GGAs, unlike AP-1, have an absolute requirement for this dileucine motif to bind their cargo. This is consistent with the possibility that the GGAs play a role in the retrograde trafficking of the MPRs. However, because the CI-MPR and AP-1 colocalize in the early endosomes in the absence of GGAs, it is not clear that the GGAs serve to usher the receptors into AP-1 CCVs at this location. Another cytosolic protein, phosphofurin acidic cluster sorting protein 1, has been proposed to perform this function at the endosome (Crump et al., 2001).

The finding that GGA knockdown results in morphologic alterations of the trans-Golgi and TGN extends the reports that overexpression of the various GGAs causes structural changes in the Golgi (Poussu et al., 2000; Takatsu et al., 2000). In addition, it has been reported that expression of a dominant-negative mutant of BIG2, an ARF-guanine nucleotide exchange factor that acts at the trans-Golgi/TGN, results in redistribution of GGA1 and AP-1 to the cytosol and membrane tubulation of the TGN (Shinotsuka et al., 2002). Golgi localization of COPI remained unchanged, and the rest of the Golgi architecture was preserved. Although this phenotype exhibits similarities to the GGA knockdown cells, it differs in that the CI-MPR was found on the tubules emanating from the Golgi region rather than on EEA1-positive structures, as observed in our experiments. The distribution of β-GalT was not analyzed in that experiment, so it is uncertain whether the trans-Golgi was affected. However, TGN46 distribution was unaltered, indicating that the BIG2 dominant-negative mutant induced a selective alteration in TGN morphology. Further analyses are needed to decipher the exact role of the GGAs in maintaining Golgi morphology.

Finally, it should be noted that the GGAs, in addition to interacting with each other, also bind to AP-1 (Doray et al., 2002c). In this case, the hinge regions of the GGAs bind to the γ-appendage of AP-1. Dissociation of GGA1 and GGA3 from AP-1 is mediated by phosphorylation of the GGA hinge domains by a casein kinase 2 that is associated with AP-1. It will be important to determine if the various phosphorylation sites on GGA1 and GGA3 regulate the formation and dissolution of the complexes that form on the Golgi membrane.

Materials and methods

Materials

Glutathione-Sepharose 4B beads were purchased from Amersham Biosciences; protein A-Sepharose beads were obtained from Repligen; and CN-Br activated Sepharose 4B beads and protein G-Sepharose beads were purchased from Sigma-Aldrich. MG132 was purchased from Calbiochem. Tissue culture medium was purchased from Invitrogen, and protease inhibitor cocktail tablets were purchased from Roche. Metabolic labeling was performed using Translabel® [^{35}S]methionine:cysteine (70:30) from ICN Biomedicals. All other chemicals used were analytical grade obtained from Sigma-Aldrich.

Antibodies

Antibodies were obtained from Santa Cruz Biotechnology, Inc. as follows: mouse monoclonal and rabbit polyclonal anti-c-myc antibodies; mouse monoclonal and rabbit polyclonal anti-HA antibodies; mouse monoclonal anti-TGN-38 and goat polyclonal anti-actin antibody. Mouse mAbs to GGA3, EEA1, and to AP-1γ and rabbit pAbs to giantin were purchased from BD Biosciences. Rabbit polyclonal anti-p63 antibody, rabbit polyclonal anti-GGA1 antibody, and mouse monoclonal anti-β 1–4 galactosyltransferase antibodies were gifts from Jack Rohrer (University of Zurich, Zurich, Switzerland), Margaret S. Robinson (University of Cambridge, Cambridge, UK), and Eric G. Berger, (University of Zurich), respectively. Affinity-purified rabbit polyclonal anti-CI-MPR antibody and rabbit anti–human cathepsin D antisera were obtained from Walter Gregory of the Kornfeld laboratory. Rabbit polyclonal anti-GGA1 and anti-GGA2 antibodies were generated against myc-GGA1 and GGA2-HA expressed and purified from SF9 extracts (Ghosh and Kornfeld, 2003). The sera were purified over affinity columns made by coupling GST-GGA1 or GST-GGA2 to CN-Br activated Sepharose 4B beads. Alexa® Fluor–conjugated secondary antibodies for immunofluorescence were obtained from Molecular Probes, Inc., and species-specific HRP-conjugated secondary antibodies used for Western blotting were purchased from Amersham Biosciences.

Buffers

Buffer A consisted of PBS supplemented with 1 mg/ml BSA and 0.2% Triton X-100. Buffer B consisted of 20 mM Hepes-KOH, pH 7.2, 5 mM magnesium acetate, 125 mM potassium acetate, 0.1% Triton X-100, and 1 mM

DTT. Buffer C consisted of 25 mM Hepes-KOH, pH 7.2, 125 mM potassium acetate, 2.5 mM magnesium acetate, 1 mM DTT, and 0.4% Triton X-100. Buffer D consisted of 0.1 M Tris, pH 8.0, 0.1 M NaCl, 0.5% sodium deoxycholate, 0.2% SDS, and 1% Triton X-100.

RNAi

The p-Super vector system (Brummelkamp et al., 2002) that directs synthesis of siRNAs in mammalian cells was used in all experiments. The siRNA targets were found on GGAs 1, 2, and 3 using the oligo designing tool (Ambion). The targets chosen for RNAi were as follows: position 463 of the human GGA1-gene ^{463}AAGCTTCCAGATGACACTACC^{483}, position 1428 of the human GGA2-gene ^{1428}AATACACCTCTGGCTCAAGTG^{1448}, and position 356 of the human GGA3-gene ^{356}AATTCCTGTGGATAGGACGCT^{376}. Forward and reverse primers designed for these sequences were synthesized by Invitrogen. The resultant 64-mer oligos were phosphorylated before ligation using T4 kinase (GIBCO BRL). The plasmid DNA encoding the vector was digested with HindIII and BglII for cloning in the 64-bp inserts. After ligation, the DNA was transformed into XL1-Blue competent cells (Stratagene) as described in the manufacturer's protocol. Colonies were screened for the presence or absence of the inserts by PCR, which was confirmed by sequencing of the DNA. DNA used in HeLa cell transfections was made with a Maxiprep kit (Qiagen) as described in the manufacturer's protocol. Plasmid DNA encoding p-Super vector with inserts targeting AP-1γ was a gift from Alex Ungewickell (Washington University School of Medicine).

For rescue assays (Fig. 5 and Fig. 10), adenine at position 471 (within the target siRNA sequence) in the nucleotide sequence of the construct myc-GGA1 was mutated to cytidine to achieve RNAi resistance without changing the encoded amino acid.

Tissue culture and transient and stable transfections

HeLa cells were grown in Dulbecco's modification of minimal essential medium supplemented with 10% FBS, 100 U/ml penicillin, and 100 μg/ml streptomycin at 37°C in the presence of 5% CO_2. Transient and stable transfections were performed using LipofectAMINE™ plus as described in the manufacturer's protocol. When myc-GGA1 and GGA2-HA were cotransfected (Fig. 1), the ratio of the two plasmid DNAs was 1:1. In rescue assays (Fig. 10), the ratio of p-Super/RNAi plasmid DNA to pcDNA3.1-myc-GGA1 was 4:1. Hours post-transfection denotes the number of hours after removal of complexes from the monolayer cultures. Stable GGA1 and GGA2 knockdown cell lines were made by cotransfecting HeLa cells with p-Super/RNAi plasmid DNA and pBabe retroviral vector encoding puromycin resistance cassette at a ratio of 1:8. The cells were trypsinized and plated in fresh medium 24 h after transfection, and at 48 h, the medium was supplemented with 5 μg/ml of Puromycin (Sigma-Aldrich). Colonies appeared at 2–3 wk, and several clones were tested for efficiency of knockdown by Western blotting. Clones with significant knockdown (~70% decrease) in the levels of GGA1 and GGA2 were used in subsequent experiments. We were unable to select clones with complete silencing of either GGA, perhaps due to nonviability of such cells.

Plasmids and protein expression

Myc-tagged GGA1 and GGA2-HA wild-type plasmids were obtained as described previously (Doray et al., 2002b). Bacmid DNAs were transfected into SF9 insect cells to produce recombinant baculoviruses that were amplified and used to express the various GGAs in the insect cells as described before (Doray et al., 2002b). Insect cells expressing the GGA proteins were routinely harvested 48 h after infection, lysed into cold buffer C supplemented with protease inhibitor cocktail by sonication, and centrifuged at 20,000 *g* for 10 min. The supernatant containing the GGA protein was stored at −80°C. Affinity purification of myc-GGA1 wild type, myc-GGA1 D358A, GGA2-HA, and myc-GGA3 was performed as described previously (Doray et al., 2002c). Bovine adrenal cytosol was prepared as described before (Ghosh and Kornfeld, 2003).

Constructs expressing GST-GGA1fl and GST-GGA3fl were prepared by digesting myc-GGA1pFB1 and myc-GGA3pFB1 (Doray et al., 2002b) with SalI and NotI. The resultant fragments encoding GGA1 and GGA3 cDNAs were ligated with pGEX-5X-3 digested with the same enzymes. Plasmids encoding GST-GGA2, GST-GGA2-VHS (residues 29–188), GST-GGA2-VHS+GAT (residues 29–326), GST-GGA2flΔear (residues 29–479), GST-GGA2 ear (residues 473–613; Zhu et al., 2001), and GST-AP-1γ appendage (residues 703–822; Doray et al., 2002c) fusion proteins were used to express these proteins in the *Escherichia coli* strain BL21 (RIL; Stratagene) as described before (Doray et al., 2002b). The expressed proteins were coupled to glutathione-Sepharose 4B (Amersham Biosciences) as described previously (Doray et al., 2002b).

Immunofluorescence microscopy

HeLa cells were plated onto coverslips 32 h after transfection, and at ~52–54 h after transfection were fixed in 3.7% formaldehyde in PBS for 15 min at RT. The fixed cells were briefly washed with PBS to remove excess formaldehyde. Primary antibodies were used at the following dilutions in buffer A: anti-CI-MPR (rabbit polyclonal, 1:500, 4–5 μg/ml), anti-β-GalT (mouse monoclonal, 1:20), anti c-myc (mouse monoclonal, 1:100, 1–4 μg/ml), anti-HA (mouse monoclonal, 1:100, 1–4 μg/ml), anti-c-myc (rabbit polyclonal, 1:250, 1–2 μg/ml), anti-HA (rabbit polyclonal, 1:250, 1–2 μg/ml), anti-giantin (rabbit polyclonal, 1:2,000), anti-GGA1 (rabbit polyclonal, 1:50), anti -GGA2 (rabbit polyclonal, 1:100), anti-GGA3 (mouse monoclonal, 1:100), anti-AP-1γ (mouse monoclonal, 1:250), and anti-EEA1 (mouse monoclonal, 1:300). Incubations with primary antibodies were performed at RT for 60 min. After three 10-min washes with PBS, the cells were incubated with secondary antibodies at a dilution of 1:500 in buffer A for 60 min at RT in the dark. Washes were performed as before and the coverslips were dried and mounted in Gel/Mount anti-fade aqueous mounting medium (Biomedia Corporation). The slides were viewed with an Eclipse fluorescence microscope (model E-800; Nikon), and images were acquired using a Magnafire camera system from Optronics. For confocal imaging, Alexa® Fluor–488 and –568 fluorescences were viewed with a confocal/multiphoton laser scanning imaging system (MRC-1024; Bio-Rad Laboratories) based on a microscope (model BX50WI; Olympus) using a krypton/argon laser with excitation wavelengths of 488 and 568 nm, respectively. Images were acquired using LaserSharp (Bio-Rad Laboratories), and the Bio-Rad confocal PIC format image z-series stacks were merged using Confocal Assistant, v4.02. The colocalization coefficients were calculated using MetaMorph® software, v.4.6, from Universal Imaging Corp.

Cryo-immunogold EM

For immuno-EM, L cells expressing GGA1-myc were fixed with 0.2% glutaraldehyde plus 2% PFA in 0.1 M sodium phosphate buffer at pH 7.4. Control and GGA1 siRNA HeLa cells were fixed with 4% PFA in the same buffer. Cells were stored in 1% PFA until use. Cells were washed in buffer, pelleted by centrifugation, and embedded in 10% gelatin. Gelatin blocks with cells were infused with 2.3 M sucrose and frozen in liquid nitrogen. Cryosectioning and immunogold labeling have been described before (Geuze et al., 1981; Raposo et al., 1997). Double- and triple-immunogold labeling sequences together with the respective protein A-gold particle sizes are indicated in Fig. 2. To estimate colocalization of GGAs on individual CCVs and buds at the TGN, GGA-labeled coated vesicles and buds were counted in triple-labeled sections of myc-GGA1–expressing cells and categorized as single-, double-, or triple-labeled. GGAs 1, 2, and 3 were labeled with gold particles of 15, 10, and 5 nm, respectively. A total of 202 buds and vesicles in 20 electron micrographs of trans-Golgi areas at 25,000× were counted. Countings of CI-MPR gold particles was done as described in Table I.

Binding assays

The binding assays contained 100 μg purified GST-fusion ligand prebound to glutathione-Sepharose beads at RT for 2 h and 2 μg immunopurified GGAs (myc-GGA1 wt, myc-GGA1 D358A, GGA2-HA, and myc-GGA3; Fig. 3) in a final volume of 350 μl buffer B. The reactions were incubated at 4°C for 4 h with constant tumbling. The beads were then collected by centrifugation at 3,000 rpm and were given four washes, each with 1 ml buffer B. The pellet was then boiled in SDS sample buffer. Unless otherwise specified, 20% of the pellet and 2% of the supernatant/input was subjected to SDS-PAGE followed by Western blotting.

Cross-linking and coimmunoprecipitation

Recruitment assays were performed with or without GTPγS as described previously (Drake et al., 2000). A similar assay scaled up to 8 ml volume was used for the cross-linking experiment (Fig. 4). In brief, recruitment reactions were performed at 37°C for 30 min. Reactions were terminated by rapid cooling at 4°C followed by centrifugation at 14,000 *g* for 15 min. The supernatants were removed and saved. The membrane pellets were resuspended in PBS after a brief wash with buffer B. Cytosol and resuspended membrane fractions were cross-linked for 2 h on ice using DTSSP as described in the manufacturer's protocol. Another identical set was subjected to a similar incubation in the absence of DTSSP. Individual reactions were terminated by the addition of 1 M Tris-Cl, pH 7.5, followed by an additional 15 min of quenching. Membrane-associated complexes were solubilized using 0.4% Triton X-100 and subjected to sonication (six 5 s pulses at a setting of 3 on Fisher dismembrator, model 550). Insoluble membrane components were removed by centrifugation at 14,000 *g* for 15 min. The supernatant was used for immunoprecipitation of GGAs 1 and 2 at 4°C

overnight with tumbling. Protein A agarose beads were added the following morning and were allowed to mix for 1 h at 4°C. The beads were centrifuged at 3,000 *g* and washed four times with 1 ml buffer B. Bound proteins were eluted by boiling in SDS sample buffer and subjected to SDS-PAGE followed by immunoblotting.

Western blotting

Samples boiled in SDS sample buffer were subjected to SDS-PAGE on a 10% gel, transferred onto nitrocellulose, and immunoblotted with the antibodies mentioned before. The blot was developed using an ECL detection kit from Amersham Biosciences, and was filmed with X-OMAT K (Kodak).

Cathepsin D sorting assays

Metabolic labeling and sorting of cathepsin D by the various GGA knockdown cell lines was performed as described previously (Doray et al., 2002a).

We thank Agami Reuven and Anton Berns (The Netherlands Cancer Institute, Antoni Van Leeuwenhoek Hospital, Amsterdam, Netherlands) for the P-super vector, Balraj Doray (Washington University School of Medicine) for plasmids expressing GST-GGA1 fl and GST-GGA3 fl, Alex Ungewickell for helpful guidance with RNAi, Andrey Frolov for skillful assistance with confocal microscopy and image analysis, and Rene Scriwanek and Marc van Peski for their excellent help in preparing the micrographs. We thank Rosalind Kornfeld and Balraj Doray for critical reading of the manuscript.

This work was supported by National Institutes of Health grant RO1 CA-08759 (to S. Kornfeld).

Submitted: 8 August 2003
Accepted: 25 September 2003

References

Black, M.W., and H.R. Pelham. 2000. A selective transport route from Golgi to late endosomes that requires the yeast GGA proteins. *J. Cell Biol.* 151:587–600.

Boman, A.L., C. Zhang, X. Zhu, and R.A. Kahn. 2000. A family of ADP-ribosylation factor effectors that can alter membrane transport through the trans-Golgi. *Mol. Biol. Cell.* 11:1241–1255.

Brummelkamp, T.R., R. Bernards, and R. Agami. 2002. A system for stable expression of short interfering RNAs in mammalian cells. *Science.* 296:550–553.

Crump, C.M., Y. Xiang, L. Thomas, F. Gu, C. Austin, S.A. Tooze, and G. Thomas. 2001. PACS-1 binding to adaptors is required for acidic cluster motif-mediated protein traffic. *EMBO J.* 20:2191–2201.

Dell'Angelica, E.C., R. Puertollano, C. Mullins, R.C. Aguilar, J.D. Vargas, L.M. Hartnell, and J.S. Bonifacino. 2000. GGAs: a family of ADP ribosylation factor-binding proteins related to adaptors and associated with the Golgi complex. *J. Cell Biol.* 149:81–94.

Doray, B., K. Bruns, P. Ghosh, and S. Kornfeld. 2002a. Interaction of the cation-dependent mannose 6-phosphate receptor with GGA proteins. *J. Biol. Chem.* 277:18477–18482.

Doray, B., K. Bruns, P. Ghosh, and S.A. Kornfeld. 2002b. Autoinhibition of the ligand-binding site of GGA1/3 VHS domains by an internal acidic cluster-dileucine motif. *Proc. Natl. Acad. Sci. USA.* 99:8072–8077.

Doray, B., P. Ghosh, J. Griffith, H.J. Geuze, and S. Kornfeld. 2002c. Cooperation of GGAs and AP-1 in packaging MPRs at the trans-Golgi network. *Science.* 297:1700–1703.

Drake, M.T., Y. Zhu, and S. Kornfeld. 2000. The assembly of AP-3 adaptor complex-containing clathrin-coated vesicles on synthetic liposomes. *Mol. Biol. Cell.* 11:3723–3736.

Geuze, H.J., J.W. Slot, P.A. van der Ley, and R.C.T. Scheffer. 1981. Use of colloidal gold particles in double-labeling immunoelectron microscopy of ultrathin frozen tissue sections. *J. Cell Biol.* 89:653–665.

Ghosh, P., and S. Kornfeld. 2003. Phosphorylation-induced conformational changes regulate GGAs 1 and 3 function at the trans-Golgi network. *J. Biol. Chem.* 278:14543–14549.

Hirst, J., W.W. Lui, N.A. Bright, N. Totty, M.N. Seaman, and M.S. Robinson. 2000. A family of proteins with γ-adaptin and VHS domains that facilitate trafficking between the trans-Golgi network and the vacuole/lysosome. *J. Cell Biol.* 149:67–80.

Hirst, J., A. Motley, K. Harasaki, S.Y. Peak Chew, and M.S. Robinson. 2003. EpsinR: an ENTH domain-containing protein that interacts with AP-1. *Mol. Biol. Cell.* 14:625–641.

Martinez-Menarguez, J.A., R. Prekeris, V.M. Oorschot, R. Scheller, J.W. Slot, H.J. Geuze, and J. Klumperman. 2001. Peri-Golgi vesicles contain retrograde but not antegrade proteins consistent with the cisternal progression model of intra-Golgi transport. *J. Cell Biol.* 155:1213–1224.

Meyer, C., D. Zizioli, S. Lausmann, E.L. Eskelinen, J. Hamann, P. Saftig, K. von Figura, and P. Schu. 2000. mu1A-adaptin-deficient mice: lethality, loss of AP-1 binding and rerouting of mannose 6-phosphate receptors. *EMBO J.* 19:2193–2203.

Meyer, C., E.L. Eskelinen, M.R. Guruprasad, K. von Figura, and P. Schu. 2001. Mu 1A deficiency induces a profound increase in MPR300/IGF-II receptor internalization rate. *J. Cell Sci.* 114:4469–4476.

Misra, S., R. Puertollano, Y. Kato, J.S. Bonifacino, and J.H. Hurley. 2002. Structural basis for acidic-cluster-dileucine sorting-signal recognition by VHS domains. *Nature.* 415:933–937.

Nilsson, T., M. Pypaert, M.H. Hoe, P. Slusarewicz, E.G. Berger, and G. Warren. 1993. Overlapping distribution of two glycosyltransferases in the Golgi apparatus of HeLa cells. *J. Cell Biol.* 120:5–13.

Poussu, A., O. Lohi, and V.P. Lehto. 2000. Vear, a novel Golgi-associated protein with VHS and γ-adaptin "ear" domains. *J. Biol. Chem.* 275:7176–7183.

Poussu, A.M., P.H. Thompson, M.J. Makinen, and V.P. Lehto. 2001. Vear, a novel Golgi-associated protein, is preferentially expressed in type I cells in skeletal muscle. *Muscle Nerve.* 24:127–129.

Puertollano, R., R.C. Aguilar, I. Gorshkova, R.J. Crouch, and J.S. Bonifacino. 2001. Sorting of mannose 6-phosphate receptors mediated by the GGAs. *Science.* 292:1712–1716.

Puertollano, R., N.N. van der Wel, L.E. Greene, E. Eisenberg, P.J. Peters, and J.S. Bonifacino. 2003. Morphology and dynamics of clathrin/GGA1-coated carriers budding from the trans-Golgi network. *Mol. Biol. Cell.* 14:1545–1557.

Raposo, G., M.J. Kleijmeer, G. Posthuma, J.W. Slot, and H.J. Geuze. 1997. Immunogold labeling of ultrathin cryosections: application in immunology. *In* Weir's Handbook of Experimental Immunology. Fifth edition. L.A. Herzenberg, D.M. Weir, and C. Blackwell, editors. Blackwell Science, Malden, MA. 208.1–208.11.

Shiba, T., H. Takatsu, T. Nogi, N. Matsugaki, M. Kawasaki, N. Igarashi, M. Suzuki, R. Kato, T. Earnest, K. Nakayama, and S. Wakatsuki. 2002. Structural basis for recognition of acidic-cluster dileucine sequence by GGA1. *Nature.* 415:937–941.

Shinotsuka, C., S. Waguri, M. Wakasugi, Y. Uchiyama, and K. Nakayama. 2002. Dominant-negative mutant of BIG2, an ARF-guanine nucleotide exchange factor, specifically affects membrane trafficking from the trans-Golgi network through inhibiting membrane association of AP-1 and GGA coat proteins. *Biochem. Biophys. Res. Commun.* 294:254–260.

Strous, G.J., P. van Kerkhof, R. Willemsen, H.J. Geuze, and E.G. Berger. 1983. Transport and topology of galactosyltransferase in endomembranes of HeLa cells. *J. Cell Biol.* 97:723–727.

Stults, N.L., M. Fechheimer, and R.D. Cummings. 1989. Relationship between Golgi architecture and glycoprotein biosynthesis and transport in Chinese hamster ovary cells. *J. Biol. Chem.* 264:19956–19966.

Suer, S., S. Misra, L.F. Saidi, and J.H. Hurley. 2003. Structure of the GAT domain of human GGA1: A syntaxin amino-terminal domain fold in an endosomal trafficking adaptor. *Proc. Natl. Acad. Sci. USA.* 100:4451–4456.

Takatsu, H., K. Yoshino, and K. Nakayama. 2000. Adaptor γ ear homology domain conserved in γ-adaptin and GGA proteins that interact with γ-synergin. *Biochem. Biophys. Res. Commun.* 271:719–725.

Takatsu, H., Y. Katoh, Y. Shiba, and K. Nakayama. 2001. Golgi-localizing, gamma-adaptin ear homology domain, ADP-ribosylation factor-binding (GGA) proteins interact with acidic dileucine sequences within the cytoplasmic domains of sorting receptors through their Vps27p/Hrs/STAM (VHS) domains. *J. Biol. Chem.* 276:28541–28545.

Tikkanen, R., S. Obermuller, K. Denzer, R. Pungitore, H.J. Geuze, K. von Figura, and S. Honing. 2000. The dileucine motif within the tail of MPR46 is required for sorting of the receptor in endosomes. *Traffic.* 1:631–640.

Wakasugi, M., S. Waguri, S. Kametaka, Y. Tomiyama, S. Kanamori, Y. Shiba, K. Nakayama, and Y. Uchiyama. 2003. Predominant expression of the short form of GGA3 in human cell lines and tissues. *Biochem. Biophys. Res. Commun.* 306:687–692.

Zhu, G., X. He, P. Zhai, S. Terzyan, J. Tang, and X.C. Zhang. 2003. Crystal structure of GGA2 VHS domain and its implication in plasticity in the ligand binding pocket. *FEBS Lett.* 537:171–176.

Zhu, Y., B. Doray, A. Poussu, V.P. Lehto, and S. Kornfeld. 2001. Binding of GGA2 to the lysosomal enzyme sorting motif of the mannose 6-phosphate receptor. *Science.* 292:1716–1718.